

Data Descriptor

An interactive enhanced driving dataset for autonomous driving

Authors

Haojie Feng¹, Peizhi Zhang¹, Mengjie Tian¹, Xinrui Zhang¹, Zhuoren Li¹, Junpeng Huang¹, Xiurong Wang¹, Junfan Zhu³, Jianzhou Wang⁴, Dongxiao Yin², Lu Xiong¹

Affiliations

1. School of Automotive Studies, Tongji University, Shanghai, 201804, China
2. Tongji Automotive Design & Research Institute Co., Ltd., Shanghai, 201804, China
3. University of Chicago, Chicago, IL 60637, USA
4. Faculty of Computer Science, University of New Brunswick, Fredericton, NB E3B 5A3, Canada

corresponding author(s): Peizhi Zhang (zhangpeizhitom@126.com)

Abstract:

The evolution of autonomous driving towards full automation demands robust interactive capabilities; however, the development of Vision-Language-Action (VLA) models is constrained by the sparsity of interactive scenarios and inadequate multimodal alignment in existing data. To this end, this paper proposes the Interactive Enhanced Driving Dataset (IEDD). We develop a scalable pipeline to mine million-level interactive segments from naturalistic driving data based on interactive trajectories, and design metrics to quantify the interaction processes. Furthermore, the IEDD-VQA dataset is constructed by generating synthetic Bird's Eye View (BEV) videos where semantic actions are strictly aligned with structured language. Benchmark results evaluating ten mainstream Vision Language Models (VLMs) are provided to demonstrate the dataset's reuse value in assessing and fine-tuning the reasoning capabilities of autonomous driving models.

Background & Summary

Autonomous driving technology has emerged as a transformative force in modern transportation, promising to fundamentally reshape road safety and traffic efficiency. As vehicles evolve from basic driver assistance systems toward full automation, their navigability in complex dynamic environments increasingly depends on the capability for robust interaction with other road users, such as pedestrians and non-motorized vehicles. However, interaction scenarios involving lane changes, intersection negotiations, and

crosswalk yielding¹ constitute critical challenges to the safety and efficiency of current systems. A recent matched case-control study quantitatively revealed this shortcoming:² although automated driving systems demonstrate advantages in routine scenarios, their accident risk is 1.98 times that of human-driven vehicles in turning scenarios involving complex negotiations; furthermore, under lighting conditions with high perception demands, such as dawn or dusk, this risk disparity widens to 5.25 times. These data intuitively indicate that precise perception, intention prediction, and decision-making responses regarding such interactive behaviors remain bottlenecks that must be overcome to achieve high-level intelligent driving.³

Recent progress in autonomous driving research has shifted towards the Vision-Language-Action (VLA) paradigm.⁴ Its core lies in utilizing Vision Language Models (VLMs)⁵ or Large Language Models (LLMs) to achieve a human-like understanding of driving scenarios by integrating visual perception with semantic logical reasoning. Representative works include Li Auto's DriveVLM, LatentVLA, and ReflectDrive,⁶⁻⁸ XPeng's FastDriveVLA,⁹ and Waymo's EMMA, S4-Driver, and MotionLM.¹⁰⁻¹² Unlike traditional data-driven methods that rely solely on trajectory or sensor data, VLM frameworks require rich multi-modal inputs (encompassing visual prompts, contextual semantics, and natural language descriptions) to simulate a human driver's intuitive understanding of interaction dynamics. However, due to the current scarcity of training data targeting VLM interaction scenarios, the development and validation of such models are severely constrained.

The primary limitation lies in the sparsity of high-quality interaction scenarios within existing datasets. Most naturalistic datasets originating from real-world driving environments, such as NGSIM¹³, nuScenes¹⁴, Lyft Level 5¹⁵, and the Waymo Open Motion Dataset¹⁶, primarily capture routine, non-interactive driving behaviors, whereas critical interaction events (e.g., merging in congested traffic, yielding to emergency vehicles) belong to a relatively rare long-tail distribution¹⁷. Identifying and extracting these sparse yet meaningful interaction events from massive amounts of data is a highly challenging task. Furthermore, existing datasets (e.g., KITTI¹⁸, BDD100K¹⁹, ONCE²⁰) mostly focus on a single modality, typically containing only visual information (images, point clouds) or trajectory data (position, velocity, acceleration), and lack crucial language annotations²¹⁻²⁴ (such as driver intention descriptions and scenario context). This absence of multi-modal data severely hinders VLMs from learning comprehensive interactive driving representations aligned with human cognition, thereby limiting their performance in real-world traffic environments.

The acquisition and management of multi-modal driving data are inherently time-consuming and resource-intensive, typically involving the deployment of specialized hardware, large-scale collection campaigns, and labor-intensive manual annotation. In light of this, developing a low-cost approach to enhance existing datasets, rather than constructing new ones from scratch, represents a pragmatic and efficient strategy. To bridge the aforementioned gap, this study proposes a novel framework: extracting ego-vehicle-centric interaction scenarios from public trajectory datasets, designing quantitative metrics for the interaction process, and synthesizing complementary visual and semantic data based on real trajectory information. Utilizing this synthesized data, testing benchmarks and fine-tuning enhancements tailored to the interaction domain can be provided for autonomous driving VLMs. The main contributions of this paper are as follows:

- Constructed a million-level heterogeneous interactive enhanced driving dataset (IEDD). We propose a heterogeneous trajectory homogenization and interaction mining framework, extracting and integrating over seven million ego-vehicle-centric interaction scenarios from five naturalistic driving datasets. This framework effectively overcomes the heterogeneous barriers of multi-source data and specifically breaks through the data sparsity bottleneck of high-value, complex interaction scenarios (e.g., intersection negotiations, forced merging), providing a solid data foundation for autonomous driving research.
- Developed a physics-aware multi-modal alignment and generation pipeline. We pioneer an "intensity-efficiency" dual-dimensional interaction quantification system based on interactive stochastic processes, and drive end-to-end data synthesis with these physical constraints. By strictly aligning BEV videos reconstructed from real trajectories with structured language in both spatial and temporal dimensions, we generate a high-quality vision-question-answer dataset (IEDD-VQA) encompassing counterfactual reasoning tasks, effectively bridging the gap in logical consistency present in existing data.
- Established a hierarchical evaluation benchmark and validated the domain adaptation paradigm. We establish a hierarchical VLM evaluation benchmark encompassing perception, description, quantification, and counterfactual reasoning (L1-L4), and systematically evaluate ten mainstream large multi-modal models. Fine-tuning experiments and ablation analyses not only reveal the inherent bottlenecks of general-purpose models in physical estimation but also demonstrate that IEDD-VQA can significantly reduce quantification errors and enhance logical reasoning capabilities, providing empirical evidence for the domain adaptation of general VLMs to autonomous driving expert models.

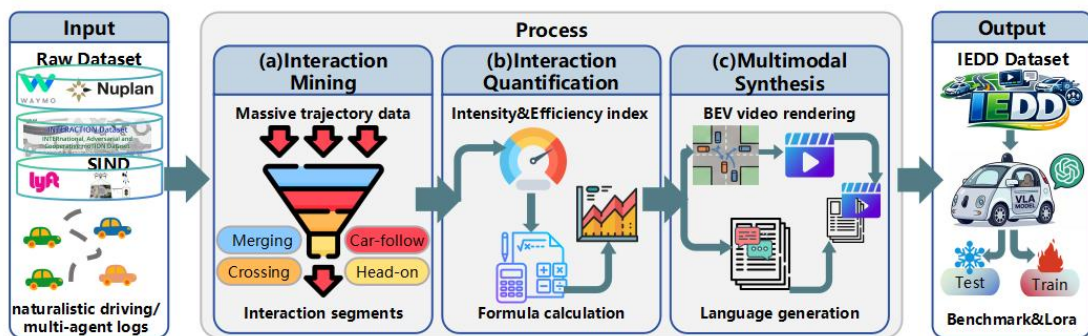


Fig 1. Overview of the entire pipeline for generating the IEDD data.

Related Works

As autonomous driving technology advances toward L4/L5 high-level automation, the decision-making capability of vehicles in dynamic and complex environments has become the core of technological breakthroughs. Among these challenges, understanding and handling unstructured negotiations and interactive behaviors with other traffic participants, such as vehicles, pedestrians, and cyclists, directly impacts the safety, compliance, and social acceptance of the system. In light of this, mining high-value interaction scenarios from massive amounts of driving data and constructing a closed-loop data system with semantic understanding capabilities have become a consensus in both academia and industry. This

section will systematically review the related research progress from three dimensions: interaction scenario mining, the current status of autonomous driving datasets, and the VLA data paradigm.

Interaction Scenario Mining and Quantification Methods. Autonomous vehicles frequently engage in interactions with various traffic participants on complex urban roads. These interaction events constitute highly valuable long-tail scenarios, which are crucial for enhancing model robustness. Due to the prohibitively high marginal cost of collecting high-density interaction scenarios in the real world, existing research has primarily explored two paths: scenario reconstruction and synthetic generation. Although some scholars have attempted to augment data through simulation synthesis²⁵, synthetic data often lacks the randomness and negotiation characteristics inherent in real-world driving²⁶, presenting a "Sim2Real" distribution gap, and may even degrade model performance in real-world environments due to data contamination.

In contrast, directly extracting real interaction segments from naturalistic driving data has emerged as a preferred solution that balances authenticity and cost. In recent years, researchers have proposed various extraction strategies based on physical metrics and optimization algorithms. For instance, MSAA treats interaction as a global optimization problem²⁷, utilizing the minimum change in acceleration as a core metric to screen interaction segments; PODAR introduces potential field theory²⁸, measuring interaction risks by predicting the trajectories of surrounding vehicles and estimating potential collision kinetic energy. Furthermore, VistaScenario achieves refined scenario measurement and comparison based on graph computation trees and Dynamic Time Warping (DTW)²⁹; other studies utilize interaction primitive methods to automatically extract complex multi-vehicle interaction patterns through unsupervised clustering. Moreover, some scholars model the complexity of dynamic scenarios as the sum of the complexities of interacting pairs, calculating interaction intensity based on physical quantities such as encounter angle, relative distance, and relative velocity³⁰⁻³³. Although the aforementioned methods are effective in specific scenarios, there remains a lack of a universal standard capable of uniformly quantifying interaction intensity and supporting semantic interpretation^{34,35}.

Current Status of Autonomous Driving Interaction Datasets. In recent years, large-scale autonomous driving datasets, represented by nuPlan³⁶, Lyft Level 5¹⁵, and the Waymo Open Motion Dataset¹⁶, have significantly propelled the development of perception and prediction technologies. However, these datasets are primarily designed with an orientation toward object-level perception (detection, tracking, segmentation). Despite their massive scale, they exhibit notable deficiencies in the coverage and semantic expression of interactive behaviors³⁷⁻⁴⁰. On the one hand, because simple behaviors such as driving straight dominate real-world driving, critical interaction challenges (e.g., forced merging at ramps, negotiations at unprotected intersections) are extremely sparse in the data distribution¹⁷. This sparsity makes it difficult for models to sufficiently learn strategies for mitigating long-tail risks. On the other hand, existing data lacks explicit annotations regarding decision-making rationales and interaction intentions, thereby diminishing the interpretability of the data.

Datasets specifically dedicated to interaction research are relatively scarce. The INTERACTION dataset is one of the few pioneers centered on the collection of interaction scenarios⁴¹, but its scale is relatively limited. InterHub attempts to extract interaction

segments from naturalistic driving data to supplement samples²⁷, but it lacks ego-vehicle-centric interaction measurement.

To overcome the inherent limitations of a single data collection source regarding scenario diversity and interaction density, this study adopts a cross-domain data fusion and refinement strategy. The construction of the IEDD does not start from scratch but is built upon the deep mining of existing massive naturalistic driving data. We established a set of standardized data adaptation interfaces, integrating five mainstream heterogeneous datasets, including Waymo Open Motion¹⁶, nuPlan³⁶, Lyft Level 5¹⁵, INTERACTION⁴¹, and SIND⁴². By mapping these raw trajectories—which exhibit high heterogeneity due to differences in sensor configurations, geographical locations, and traffic rules—into a unified spatio-temporal representation space, we not only inherit the scale advantages of the original datasets regarding massive perception data but also effectively circumvent their shortcoming of sparse interaction samples through targeted mining algorithms, thereby achieving an order-of-magnitude leap in the number of interaction scenarios.

Overall, although existing works have made contributions in their respective fields, the current domain still lacks a benchmark dataset that integrates "large-scale heterogeneous interaction samples," "fine-grained intensity quantification," and "rich semantic interpretation." Therefore, there remains an urgent need to construct an interaction dataset derived from naturalistic driving that covers a wider variety of interaction types and features enhanced semantic expression capabilities.

VLA Datasets and Semantic Construction for Autonomous Driving. With the evolution of Embodied AI, autonomous driving research is transitioning from modular architectures to the end-to-end VLA paradigm. In this paradigm, high-quality language labels are no longer merely descriptive texts, but rather semantic bridges connecting perceptual inputs with decision-making outputs, serving as crucial supervisory signals for realizing the closed-loop learning of "interaction understanding—logical reasoning—action execution." However, the construction of large-scale, highly reliable VLA datasets consistently faces a core contradiction between "the high cost of manual annotation" and "the hallucination noise in automated generation." Reviewing existing research, the construction strategies for language data have primarily evolved into the following three paths:

First, the expert knowledge-based manual annotation strategy. This approach prioritizes ensuring the authenticity, interpretability, and naturalness of the language. For example, the BDD-X dataset constructs high-quality explanatory texts by having individuals familiar with driving rules watch videos on Amazon Mechanical Turk as "driving instructors"⁴³ to explain driving behaviors segment by segment; the DRAMA dataset, on the other hand, insists that all question-answering pairs and captions be manually written by human annotators⁴⁴ to ensure the accuracy of descriptions for risk scenarios. Although manual annotation possesses a natural advantage in logical consistency, its prohibitively high temporal and economic costs severely limit the scalable expansion of datasets.

Second, the structured data-based template-filling strategy. To address the scalability challenge, researchers have turned to leveraging the structured information of autonomous driving data (e.g., object attributes and lane topologies). For example, NuScenes-QA innovatively models scene information as a Scene Graph⁴⁵, and by combining 66 manually designed natural language templates with a depth-first search algorithm, it achieves the

manual-free automated generation of large-scale question-answering pairs; Reason2Drive, on the other hand, adopts a "structured data template filling + GPT-4 rewriting" scheme⁴⁶, utilizing large language models to enhance linguistic diversity while relying on the underlying structured data to guarantee content accuracy. This approach achieves a compromise between consistency and scale, but it is often constrained by the rigidity of predefined templates, making it difficult to cover complex long-tail interaction logic.

Third, the hybrid pipeline strategy based on "large model generation + human verification." This is the current mainstream trend in VLA dataset construction, aiming to combine the reasoning capabilities of large models with human supervision and calibration. In practice, various variants have emerged:

Introducing Chain-of-Thought (CoT)⁴⁷ reasoning: For instance, DriveMLLM⁴⁸ and Impromptu VLA⁴⁹ guide the model to generate a CoT prior to producing question-answering pairs. By employing a two-stage pipeline of "first drafting via visual reasoning, and then summarizing into QA," they ensure that the linguistic logic extends beyond simple perceptual descriptions to encompass causal reasoning.

Graph structure and logical dependencies: DriveLM introduces the concept of graph-structured QA²¹, treating question-answer pairs as nodes and connecting the entire "perception-prediction-planning" process through logical dependencies, thereby enhancing the VLM's understanding of the driving decision-making chain.

Strict automation and verification processes: DriveAction adopts a rigorous pipeline of "LLM-based structured scene analysis + contextual QA generation + dual human verification"⁵⁰, and introduces a temporal window screening mechanism targeting keyframes, ensuring that the generated language data is highly aligned with human driving intentions.

Inspired by the aforementioned works, this paper argues that generic descriptions are inadequate to meet the negotiation demands of autonomous driving in complex dynamic scenarios. Unlike existing works that focus on static scene understanding or single-vehicle behavior descriptions, this paper advocates reconstructing the language supervision system with "interactive reasoning" at its core. Based on the extraction of high-value interaction segments from naturalistic driving data, and drawing upon the logical chain concept of DriveLM and the verification mechanism of DriveAction^{21,50}, we establish a strict mapping among physical-world interaction causality (e.g., negotiation and yielding), ego-vehicle intentions, and the linguistic logic of VLA models. This aims to address the deficiencies of existing VLA datasets in multi-vehicle negotiation and long-horizon interactive reasoning, thereby constructing an interaction-enhanced dataset with high logical consistency⁵¹⁻⁵⁶.

Methods

To construct the IEDD characterized by high interaction density and multi-modal alignment, this section proposes a scalable data production pipeline. Its overall technical architecture is illustrated in Fig 1. The pipeline consists of three tightly coupled modules: First, the interaction mining module (Fig 1a) filters and extracts four core categories of interaction segments from heterogeneous naturalistic driving datasets. Subsequently, the interaction quantification module (Fig 1b) calculates interaction intensity and efficiency metrics to assign physical attribute labels to each segment. Finally, the multi-modal synthesis module (Fig 1c)

utilizes real trajectories and behavioral rules to transform structured trajectory data into VLA training data, where visual (BEV videos) and language (QA pairs) modalities are aligned. The remainder of this section is organized as follows: First, standardized data preprocessing and scenario slicing algorithms are employed to automatically extract and classify ego-vehicle-centric interaction segments from multi-source trajectory data. Second, an interaction intensity and efficiency metric system based on stochastic processes is established to objectively quantify and grade the mined interactive behaviors. Third, based on ground-truth trajectories and quantified metrics, combined with behavioral rules, temporally and spatially strictly aligned BEV videos and structured language question-answering pairs are synthesized, thereby completing the construction of IEDD-VQA. Finally, The last section details the statistical scale, structural characteristics, and semantic content distribution of the IEDD generated through the aforementioned pipeline.

Naturalistic driving trajectory preprocessing and scenario slicing

This paper proposes a standardized automated processing pipeline aimed at efficiently mining and classifying traffic interaction scenarios from massive naturalistic driving trajectory data. Taking time-series vehicle motion states as input, this method employs four cascaded steps—trajectory preprocessing, spatio-temporal intersection detection, two-vehicle interaction classification, and multi-agent aggregation—to output a set of interaction events containing precise time windows and semantic types.

First, the raw trajectory data are cleaned and standardized. All vehicle trajectories are resampled to a time resolution of 0.1 s, and invalid zero-point data are removed. To address the issue of sudden heading angle fluctuations caused by low-speed driving or localization noise, this study calculates initial headings using the finite difference method. Subsequently, the angular sequence is decomposed into continuous signals in the angular domain and smoothed using a symmetric sliding window. Finally, the signals are mapped back to the standard angular interval, ensuring the continuity and reliability of vehicle kinematic information.

Building on this, the algorithm searches for potential trajectory intersections in the spatio-temporal dimension to identify interaction candidates. By defining spatial distance D_{search} and time difference thresholds T_{search} , an intersection is deemed valid—and its geometric center and temporal midpoint are recorded—whenever the trajectory points of two vehicles simultaneously satisfy these constraints within a spatio-temporal neighborhood. To enhance retrieval efficiency for large-scale data, the detection process utilizes a time-axis-based double-pointer sliding window mechanism, which strictly limits the search range to a specific temporal neighborhood, thereby avoiding the computational redundancy of exhaustive pairwise comparisons.

Subsequently, based on the statistical characteristics of the intersection point set, this paper employs a two-stage classification logic to subdivide interaction types. The first stage targets Car-follow behavior: when the number of trajectory overlap points is significant and the median heading difference is below a specific threshold, the interaction is classified as car-follow, and the time interval fully covering the intersection point set is defined as the event window. If the car-follow criteria are not met, the algorithm proceeds to the second stage, where events are categorized into Merging, Crossing, and Head-on based on the

relative heading angle of the two vehicles at the moment closest to the intersection. Fig 2 illustrates the spatial topological features of these different interaction types. For Merging and Crossing scenarios, the algorithm applies heading angle difference thresholds θ_{merge} and θ_{cross} to identify and extract conflict areas (indicated by yellow circles in the figure). Meanwhile, multi-agent interactions are defined as complex topologies centered on the ego-vehicle, encompassing all surrounding traffic participants with spatio-temporal overlaps. Finally, interaction time windows T_{window} are uniformly extracted to fully capture the driver's negotiation and decision-making processes.

Finally, to capture the chain reactions within complex traffic flows, the algorithm performs multi-agent interaction aggregation. Vehicles involved in multiple interaction types simultaneously within the same scene (e.g., concurrent car-follow and lane-changing) are identified as anchor points. All associated traffic participants are then recursively merged to form a unified Multi-agent Group. The effective time window for this group is defined as the global union of the time intervals of all constituent interaction events. This approach ensures the spatio-temporal and semantic integrity of complex scenarios while preventing the fragmentation of interactive behaviors.

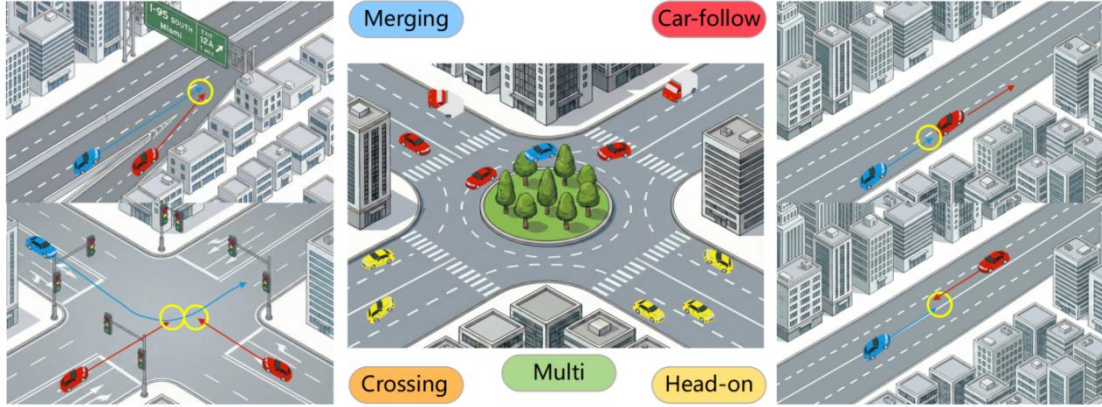


Fig 2. Schematic illustration of the geometric classification for typical interaction scenarios.

Interaction metric system based on intensity and efficiency

To evaluate the fine-grained intensity and efficiency of interaction processes, this study establishes a quantitative evaluation system based on the stochastic processes of interaction. We model vehicle-to-vehicle interactions as continuous time-series processes. By defining interaction intensity and interaction efficiency, we provide a multi-level characterization of interactive behaviors through the dual dimensions of "process risk evolution" and "decision execution quality."

(1) Interactive state space modeling

We model the interactive scenario as a stochastic process $X(t)$. For n traffic participants in the scene, the state vector $S_i(t)$ of the i -th participant at time t is defined as:

$$X(t) = \{S_1(t), S_2(t), \dots, S_n(t)\} \quad (1)$$

$$S_i(t) = [x_i(t), y_i(t), \varphi_i(t), v_i(t), a_i(t)]^T \quad (2)$$

where (x_i, y_i) represent the planar coordinates, while φ_i , v_i , and a_i denote the heading angle, velocity, and acceleration, respectively. To capture valid interaction events, we define triggering thresholds based on spatio-temporal neighborhoods: an interactive state is

identified when two vehicles simultaneously satisfy both the spatial distance threshold d_{inter} and the temporal difference threshold t_{inter} for interaction triggering.

(2) **Dynamic interaction intensity evaluation metrics**

The interaction intensity metric $Q_i(t)$ aims to quantify the instantaneous conflict pressure and the intensity of response maneuvers faced by vehicles during the interaction process. This metric is formulated as a weighted coupling of three physical components: pose adjustment, risk gradient, and environmental potential energy:

$$Q_i(t) = w_s * Q_{si}(t) + w_r * Q_{ri}(t) + w_p * Q_{pi}(t) \quad (3)$$

where w_s, w_r, w_p denote the normalized weight coefficients. Considering the significant variations in drivers' risk perception emphasis across different types of interactive scenarios, this paper adopts a category-adaptive weight allocation strategy. Specifically:

Merging Scenarios: Since merging maneuvers are highly dependent on the assessment of lane space and the potential fields of surrounding vehicles, a higher weight is assigned to the potential energy term.

Crossing Scenarios: In crossing interactions, the temporal evolution of collision risk is relatively intense; thus, the weight of the risk variation term is significantly increased to capture critical conflict moments.

Head-on Scenarios: These scenarios are typically accompanied by extremely high relative speeds. As drastic fluctuations in Time-to-Collision (TTC) and Post-Encroachment Time (PET) serve as the core indicators of danger, the risk term holds a dominant position.

This differentiated weighting scheme ensures that the quantification metrics can sensitively capture the core risk characteristics within each specific interactive pattern.

The physical definitions of each component are as follows:

(2.1) **Pose Adjustment Metric $Q_{si}(t)$:** This metric quantifies the magnitude of the kinematic response executed by the vehicle to mitigate potential conflicts. It is calculated using the normalized rate of change of velocity Δv_i and acceleration a_i :

$$Q_{si}(t) = \frac{|\Delta v_i(t)|}{v_{lim}} + \beta_Q \frac{|a_i(t)|}{a_{lim}} \quad (4)$$

where β_Q is the acceleration adjustment weight, v_{lim} denotes the vehicle speed limit, and a_{lim} represents the maximum acceleration capability. A higher value of this metric indicates that the vehicle has executed more aggressive acceleration/deceleration or maneuvering adjustments.

(2.2) **Risk Variation Metric $Q_{ri}(t)$:** This reflects the temporal evolution trend of collision risk. In contrast to static indicators that rely solely on a single instantaneous state, we introduce the time derivatives of TTC and PET to characterize the imminence of risk approach:

$$Q_{ri}(t) = \left(\frac{1}{TTC(t)} - \frac{1}{TTC(t-\Delta t)} \right) + \gamma_Q \left(\frac{1}{PET(t)} - \frac{1}{PET(t-\Delta t)} \right) \quad (5)$$

where γ_Q is the sensitivity factor for PET variation, and the difference between the two terms represents the amount of change over adjacent time steps. This formulation effectively captures critical moments of "sharp risk escalation."

(2.3) **Interactive Potential Field Metric $Q_{pi}(t)$:** This metric constructs a dynamic risk distribution based on the Artificial Potential Field (APF) method. For all surrounding

neighboring vehicles, the superimposed potential energy exerted on the ego vehicle is calculated as:

$$Q_{pi}(t) = \sum_{j \in N_i(t)} \omega_{dir}(\varphi_{ij}) * \exp[-(\frac{d_{ij}}{d_0})^2] [1 + \kappa_v * \sigma(\frac{v_{ij}^{\parallel}}{v_0})] \quad (6)$$

where $N_i(t)$ is the set of traffic participants surrounding the ego vehicle at time t , $\omega_{dir}(\cdot)$ is the direction weighting function, φ_{ij} represents the relative azimuth, d_{ij} is the relative distance between the two vehicles, d_0 is the potential field distance factor, v_0 is the relative velocity normalization factor, κ_v is the velocity sensitivity coefficient, $\sigma(\cdot)$ is the sigmoid compression function, and v_{ij}^{\parallel} is the relative approach velocity between the two vehicles.

Through the direction weighting function, the model assigns higher potential energy weights to the region in front of the ego vehicle, aligning with the human driver's perceptual characteristic of being more sensitive to frontal risks.

The interaction intensity metrics primarily focus on quantifying the dynamic risk and game-theoretic pressure during the driving process. However, in real-world traffic scenarios, optimal driving strategies involve more than mere risk avoidance; they must also achieve efficient and smooth traversal under the premise of ensuring safety. Relying solely on intensity metrics makes it difficult to comprehensively evaluate the overall quality of an interactive behavior. Therefore, to establish a complete closed-loop evaluation of interaction behavior, it is necessary to introduce a result-oriented efficiency measurement dimension.

(3) Comprehensive interaction efficiency metrics

In addition to the risk intensity during the process, evaluating the performance of interaction strategies also necessitates the consideration of the final traversal quality. This paper develops a comprehensive efficiency metric, formulated as the product of three independent dimensions—path, time, and smoothness—with a normalized range of [0,1]:

$$E_i = E_{pi} * E_{ti} * E_{si} \quad (7)$$

(3.1) **Path Consistency Metric E_{pi}** : This metric quantifies the geometric alignment between the actual trajectory and the reference path:

$$E_{pi} = \frac{d_{ref}}{d_{actual}} = \frac{\sqrt{(x_{i0} - x_{iT})^2 + (y_{i0} - y_{iT})^2}}{\int_0^T v_i(t) dt} \quad (8)$$

where the numerator represents the reference path length, and d_{ref} denotes the Euclidean distance between the starting and ending points. The denominator is the actual trajectory length. This metric reflects the vehicle's capability to adhere to the optimal trajectory during high-curvature maneuvers.

(3.2) **Time Consistency Metric E_{ti}** : This evaluates the delay penalty based on the vehicle's desired speed:

$$E_{ti} = \exp(-\alpha_E * \frac{T_{delay}}{T_{free}}) \quad (9)$$

where T_{delay} represents the cumulative time loss caused by interaction, T_{free} denotes the free-flow time, and α_E is the time sensitivity coefficient. In interactive scenarios,

strategies capable of concluding the game with minimal speed loss are assigned higher scores.

(3.3)**Driving Smoothness Metric E_{si}** : Passenger comfort is evaluated by calculating the standard deviation of acceleration within the interaction window:

$$E_{si} = \exp\left(-\beta_E * \frac{\sigma_a}{a_{normal}}\right) \quad (10)$$

where σ_a is the standard deviation of acceleration, a_{normal} denotes the acceleration normalization benchmark, and β_E represents the smoothness sensitivity coefficient. Drastic fluctuations in acceleration and deceleration result in an exponential decay of the score for this metric.

To ensure the reproducibility of the data mining and quantification processes, all key physical parameters and threshold presets involved in the interactive scenario slicing and the calculation of interaction intensity and efficiency are summarized in Table 1.

Fig 3 illustrates the physical significance of the aforementioned quantitative metrics. As the spatio-temporal distance between the two vehicles decreases (from $t=0.8s$ to $t=2.0s$), the color at the center of the environmental potential energy heatmap gradually intensifies, corresponding to a significant rise in the interaction intensity curve (as shown in the bottom-left of Fig 3). Concurrently, the bar chart in the bottom-right quantifies the traversal efficiency of different vehicles after the game-theoretic interaction, effectively distinguishing the cost differences between aggressive and conservative strategies.

In summary, the interaction intensity metric is employed to precisely locate high-risk "critical scenarios" within the long-tail distribution, while the comprehensive interaction efficiency metric serves as a reward signal to evaluate interactive traversal efficiency based on safety boundaries.

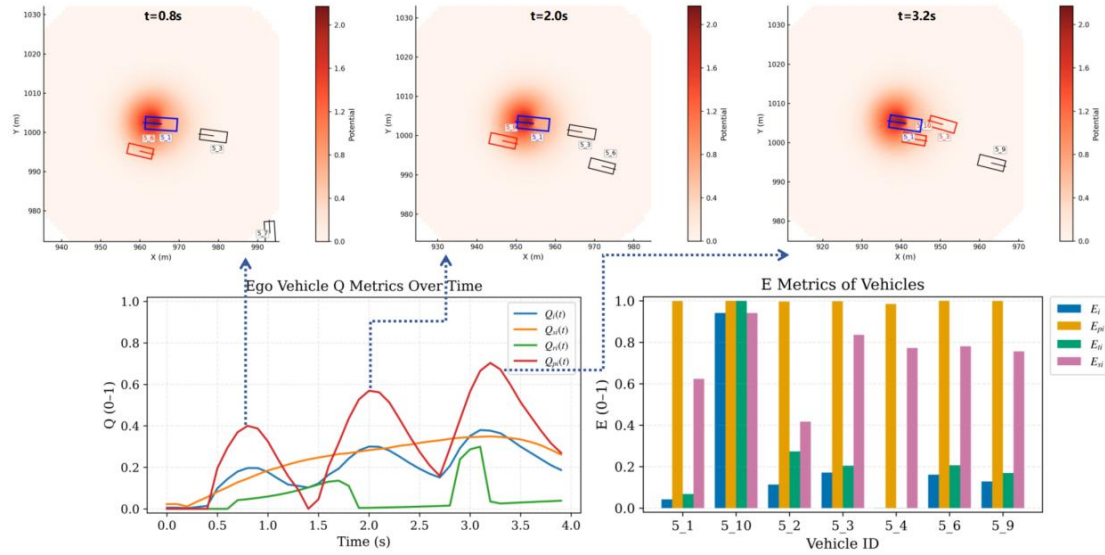


Fig 3. Spatio-temporal visualization of dynamic interaction metrics.

Category	Symbol	Description / Physical Meaning	Value

Interaction Mining	D_{search}	Spatial distance threshold for intersection search	2m
	T_{search}	Temporal difference threshold for intersection search	3s
	T_{window}	Time window for interaction event extraction	5s
	θ_{merge}	Heading angle threshold for Merging scenarios	30°
	θ_{cross}	Heading angle threshold for Crossing scenarios	160°
State Definition	d_{inter}	Interaction trigger distance threshold	50m
	t_{inter}	Interaction trigger time threshold	3s
Intensity Weights	w_s, w_r, w_p	Weight coefficients for Merging scenarios	0.25, 0.35, 0.40

	w_s, w_r, w_p	Weight coefficients for Crossing scenarios	0.20, 0.55, 0.25
	w_s, w_r, w_p	Weight coefficients for Head-on scenarios	0.15, 0.65, 0.20
Intensity Parameters	β_Q	Weight for acceleration adjustment	0.4
	v_{lim}	Speed limit normalization factor	20m/s
	a_{lim}	Maximum acceleration capacity factor	3m/s ²
	γ_Q	Sensitivity factor for PET variation	0.4
Potential Field	d_0	Effective distance factor for potential field	8
	v_0	Relative velocity normalization factor	5
	κ_v	Velocity sensitivity coefficient	1
Efficiency Metrics	α_E	Sensitivity coefficient for time efficiency	0.8

	a_{normal}	Acceleration normalization baseline	2m/s ²
	β_E	Sensitivity coefficient for driving smoothness	1.2

Table 1. Summary of Key Parameters for Interaction Mining and Quantification

Multimodal interaction instruction data generation pipeline

To address the deficiencies of current autonomous driving datasets in VLA alignment and to support end-to-end learning of complex game-theoretic behaviors, this study establishes a scalable data synthesis pipeline. Taking the interaction snippets extracted in "Naturalistic driving trajectory preprocessing and scenario slicing" and the quantitative metrics calculated in "Interaction metric system based on intensity and efficiency" as core inputs, the framework aims to generate triplet samples where visual features, structured semantics, and natural language descriptions are highly coupled. This section details the mapping mechanism from continuous trajectories to discrete semantics, the rule-constrained language generation strategy, and the implementation of cross-modal spatio-temporal alignment.

(1) Structured semantic representation and behavior serialization

To enable VLMs to comprehend continuous vehicle kinematic characteristics, trajectory data are abstracted into symbolic semantic units, forming a structured semantic set that comprises agent behavior chains, interactive relationships, and metadata.

Behavioral Atom Recognition and Temporal Compression: The continuous state space of vehicles is discretized into sequences of "behavioral atoms." First, instantaneous states are determined for each frame based on physical features such as velocity, acceleration, and yaw rate. Subsequently, to eliminate short-term fluctuations caused by sensor noise and to extract high-level semantics, a temporal aggregation strategy is employed to merge consecutive homogeneous atoms into compact "behavioral chains." This process explicitly records the start and end time windows for each action, providing precise temporal evidence for subsequent linguistic descriptions.

Interaction Relationship Modeling and Phase Partitioning: Since the behavior of a single agent cannot fully characterize the game-theoretic process, we further construct models of interactive relationships between agents. Using the peak interaction intensity as a time anchor, the interaction process is divided into three evolutionary phases: "Approach," "Interaction," and "Outcome." Within each phase, relative bearing, right-of-way, and specific interaction types are explicitly extracted to endow the data with causal logic.

Encapsulation of Explainable Metadata: To ensure data consistency, the role labels of participating agents and the quantized interaction intensity levels are encapsulated as metadata. These metadata serve as semantic constraints, ensuring that the subsequently generated linguistic descriptions remain strictly faithful to physical ground truth and avoid

ambiguous expressions.

Through the aforementioned steps, continuous and complex trajectory data are successfully parsed into discrete behavioral atoms and interaction relationships with explicit semantics. These structured semantic representations serve as a bridge connecting the physical world with the linguistic space. Building upon this structured foundation, this section will elaborate on the construction of a rule-driven generation mechanism to transform these semantic insights into high-quality, hallucination-free natural language supervision signals for guiding the training of VLA models.

(2) *Rule-driven language supervision generation mechanism*

To eliminate potential "hallucination" phenomena during the large-scale model generation process, this paper proposes a controlled text generation method driven by structured semantics. Language annotations are no longer freely generated text; instead, they are constructed based on predefined semantic slots and logical templates.

(2.1) *Intensity-Aware Semantic Mapping:* The calculated continuous interaction intensity metrics are mapped onto discrete linguistic modifiers, and interpretability is enhanced through the introduction of "evidence phrases." Specifically, the system automatically extracts micro-behavioral changes (such as sharp deceleration or heading adjustments) near peak intensity moments and converts them into specific textual descriptions.

(2.2) *Multi-Level Instruction Construction:* To accommodate various training objectives, three complementary text formats are generated: global summaries outlining interacting objects and types; standardized action chains representing the interaction process; and multi-turn question-answering (QA) instructions encompassing scene perception, intent reasoning, and policy recommendations. All QA answers are strictly extracted from structured semantics, thereby enhancing the model's generalization capabilities while ensuring factual accuracy.

While high-quality linguistic instructions empower the model to understand interaction logic, another core pillar of VLA models is visual perception. A single linguistic modality is insufficient to support the model's intuitive understanding of complex spatial relationships. To construct multimodal samples with strict image-text correspondence, visual inputs must be generated that are pixel-level aligned—both spatially and temporally—with the aforementioned trajectory ground truths. The following section details the trajectory-driven BEV video rendering and its synchronization strategy with linguistic instructions.

(3) *Trajectory-driven BEV rendering and spatio-temporal alignment*

Visual inputs utilize BEV videos reconstructed from real-world trajectories, aiming to provide the model with clear global spatial awareness and ensure strict alignment between vision and language. The choice to employ BEV rather than front-view or surround-view camera images as the primary visual modality is based on dual considerations of pipeline versatility and the completeness of interaction reasoning. First, to overcome the high heterogeneity of original data sources—specifically, the significant differences in sensor configurations across datasets (such as INTERACTION, SIND, and Waymo) and the fact that many open-source trajectory-based datasets do not include synchronized surround-view imagery—we adopt a BEV rendering scheme based on high-precision trajectory reconstruction. This strategy eliminates dependence on specific hardware, ensuring that the data generation pipeline can seamlessly migrate to any trajectory dataset, thereby maximizing

the scale expansion potential of IEDD-VQA.

Second, in complex interaction scenarios, first-person perspectives often face field-of-view limitations and object occlusions, making it difficult to fully capture the global dynamics of multi-agent games. In contrast, the BEV perspective provides an unoccluded spatial representation from a "god's-eye view," explicitly presenting the road topology and relative positional relationships of surrounding vehicles. This omnidirectional perception is crucial for VLA models to understand global interaction logic, predict potential conflicts, and plan long-term trajectories, serving as key auxiliary information that a single front-view perspective cannot replace.

(3.1)**Ego-Centric Standardized Rendering:** To normalize model inputs, all trajectories are transformed into a unified BEV coordinate system, with the origin set to the ego vehicle's pose at the peak interaction moment. Dynamic vehicles are rendered as oriented geometries, with short-term historical trajectories overlaid to provide motion cues.

(3.2)**Strict Spatio-Temporal Synchronization:** The quality of multimodal data depends on the alignment precision across modalities. We establish a unified temporal baseline to ensure that BEV video frames correspond strictly to trajectory sampling times. Crucially, critical moments and behavior intervals referenced in the linguistic descriptions are aligned with video frame indices at a pixel-level. This design enables the model to effectively map visual patterns, physical motion, and linguistic logic, facilitating true multimodal reasoning.

The specific data mapping mechanism is illustrated in Fig 4. The system first transforms continuous trajectory segments into discrete sequences of atomic actions (e.g., 'accelerate', 'turn left', 'yield'). Subsequently, these semantic labels are filled into predefined dialogue templates to generate question-answering pairs that are strictly aligned with the BEV video frames. The right side of Fig 4 shows an example of the generated JSON data, covering multiple layers of dialogue including perception, description, and reasoning.

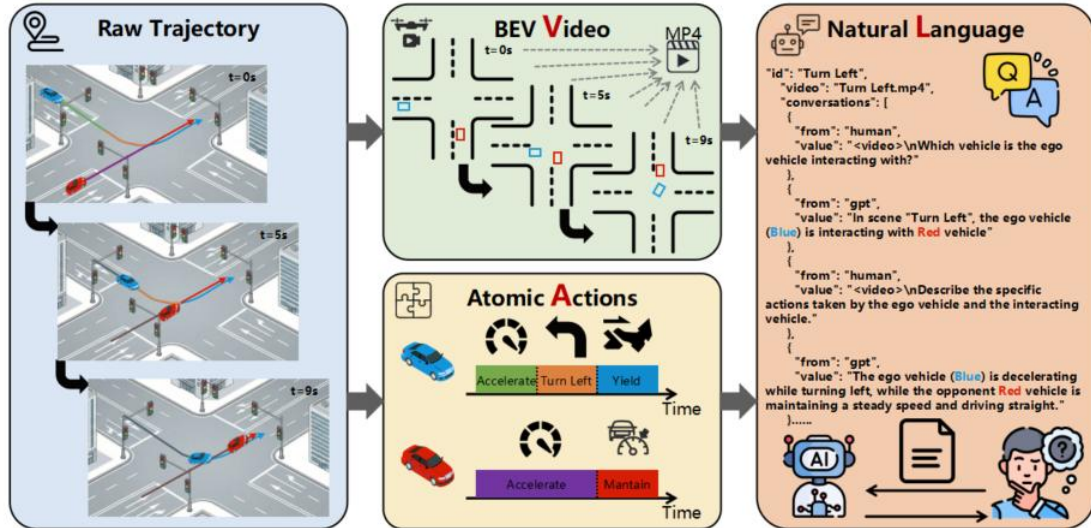


Fig 4. Trajectory-driven multimodal data synthesis workflow.

Data Records

The IEDD dataset is designed to provide multimodal, high-density, and semantically interpretable interactive driving data. Its core content comprises two primary components: a

trajectory-based large-scale interaction segment dataset (IEDD) and an instruction tuning dataset for VLA models (IEDD-VQA). This section elaborates on the statistical characteristics, storage structure, and semantic annotation specifications of the dataset.

(1) IEDD scale and statistics

To validate the advantages of IEDD in interactive scenario coverage, a systematic comparison was conducted between the proposed dataset and the original dataset. The results are summarized in Table 2.

Dataset	Head-on	Car-follow	Merging	Crossing	Two agents	Multi-agent	Amount
INTERACTION	4642	47944	15202	5267	28581	44474	73055
SIND	29546	36523	17589	37832	263	121227	121490
nuPlan	24880	44206	34464	83408	21182	165776	186958
Waymo	26428	781254	37675	59669	442314	462712	905026
Lyft	533992	714216	1284919	3494329	166296	5861160	6027456
IEDD	619488	1624143	1389849	3680505	658636	6655349	7313985

Table 2. Statistical comparison of interaction types and scales between IEDD and the original dataset.

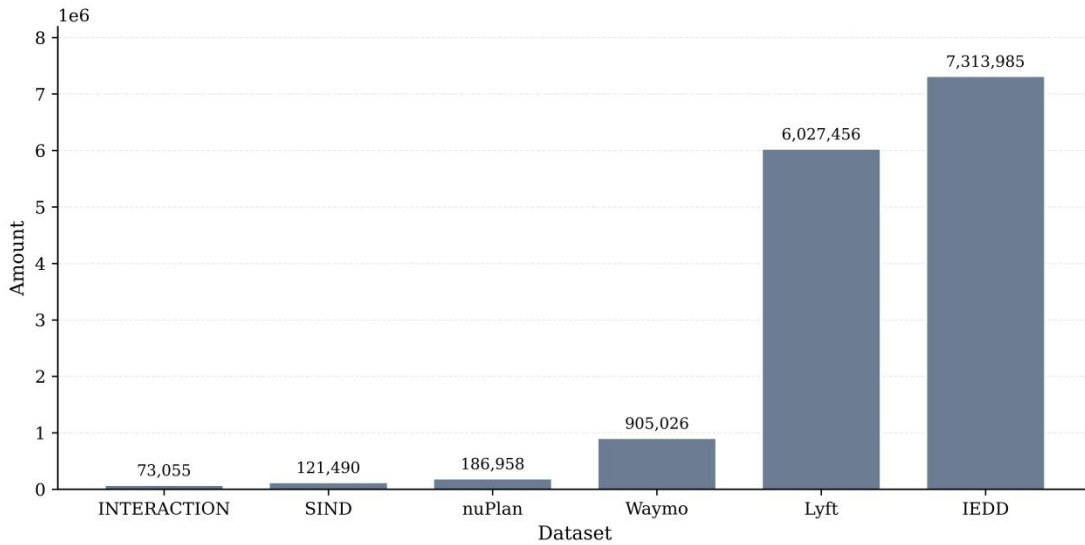


Fig 5. Comparison of total interaction segments across datasets.

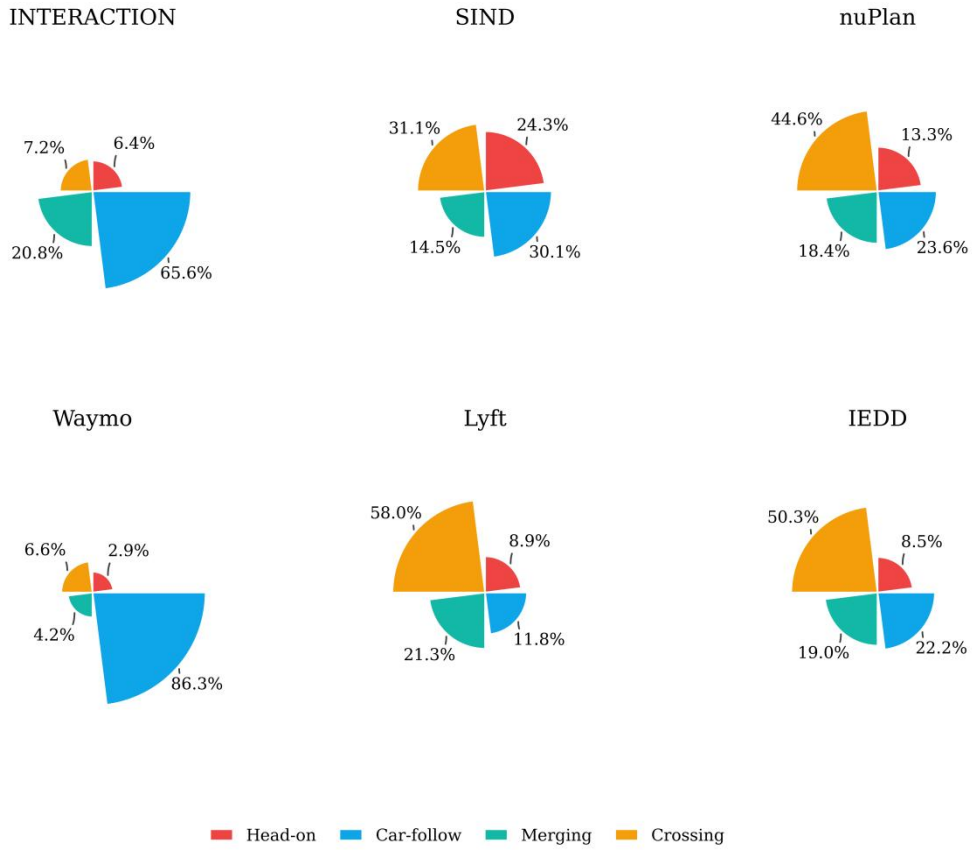


Fig 6. Pie chart comparison of interaction type distributions in IEDD.

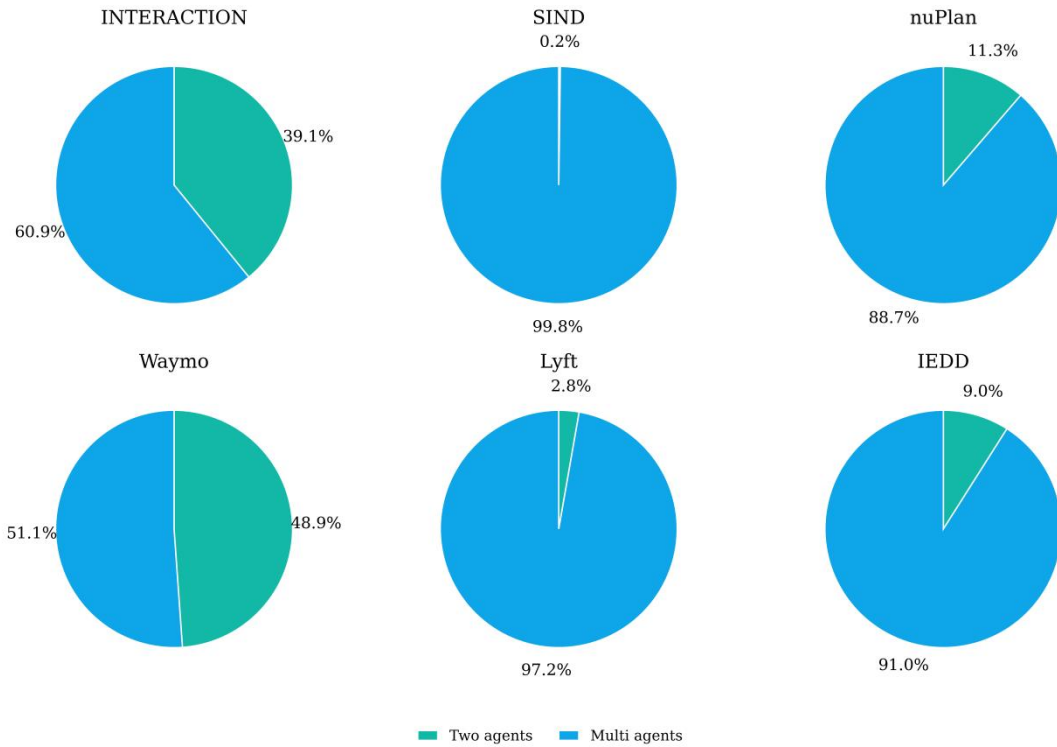


Fig 7. Proportional comparison of two-vehicle and multi-vehicle interaction scenarios in IEDD.

As illustrated in Table 2 and Fig 5, the total volume of the IEDD dataset reaches 7.31

million cases, surpassing mainstream datasets such as Lyft and Waymo in scale. More importantly, the distribution comparison in Fig 6 reveals that existing datasets (e.g., Waymo) are typically dominated by simple car-follow behaviors, whereas IEDD maintains a highly balanced distribution across long-tail high-risk scenarios, such as crossing and head-on maneuvers. Furthermore, Fig 7 highlights the most distinctive feature of this dataset: in stark contrast to SIND (where 99.8% are two-vehicle interactions), 91.0% of the samples in IEDD involve multi-agent games, thereby significantly enriching the data for complex group interactions.

(2) IEDD interaction metadata structure

The fundamental data units of IEDD are stored in the form of serialized interaction segments, designed to provide a comprehensive description ranging from macro-level scenarios to micro-level dynamics. Table 3 presents the field definitions for the interaction data. Each sample includes a unique Scene ID and a Vehicle Pair index, with the start and end Time Intervals precisely recorded. Beyond basic spatio-temporal attributes, a key feature of IEDD is the integration of quantitative indicators based on physical priors:

Q_i Over Time: The dataset records high-frequency temporal variations of the interaction intensity indicator Q_i, which directly reflect the risk fluctuations and maneuver intensity of the ego vehicle during interaction.

Multi-Vehicle Group: This defines the multi-vehicle interaction topology in complex scenarios, enabling the modeling of cascading interaction behaviors.

E_{Veh}: The passage efficiency scores of the interacting entities are recorded, providing objective ground truths for assessing decision-making quality.

Field	Description
Scene	Scenario information
Vehicle Pair	Interacting vehicle pair
Time Interval	Interaction time interval
Interaction Type	Interaction type
Q _i Over Time	Temporal variation of Q _i for the ego vehicle
Multi-Vehicle Group	Multi-vehicle interaction group
E _{Veh}	E values of involved vehicles

Table 3. Field definitions of the IEDD dataset

(3) IEDD-VQA data construction

To support end-to-end learning for Vision-Language-Action (VLA) models, high-value interaction segments were further processed into the IEDD-VQA dataset. This subset is encapsulated in a standardized JSON format, comprising BEV video paths, system prompts, and multi-turn conversations. The dataset is constructed following a "perception-description-quantization-reasoning" CoT logic. The training set specifically includes five major tasks designed around the ground-truth trajectories of the original dataset:

- **Perception and Recognition:** Identifying the interaction object IDs and their corresponding interaction types relative to the ego vehicle.
- **Behavior Description:** Requiring the model to describe the specific actions of both vehicles in natural language (e.g., "decelerating to yield" or "maintaining constant speed").
- **Physical Quantization:** Introducing numerical reasoning tasks regarding interaction intensity values and efficiency scores through a QA format.

•System Prompts: Explicitly defining that the VLM must reason from a BEV perspective based on four predefined interaction primitives.

Notably, the test set introduces a "counterfactual reasoning" task that extends beyond the training set. Fig 8 illustrates the four-level task structure of IEDD-VQA. In addition to fundamental perception and description, the yellow region in the bottom right of Fig 8 (L4 Reasoning) showcases the unique counterfactual reasoning task—requiring the model to predict potential consequences if the ego vehicle were to take a different action (e.g., accelerating instead of decelerating). This design compels the model to not only identify the current state but also comprehend the underlying causal logic of the interaction.

To ensure data rigor while evaluating high-level cognitive capabilities, this study adopts an asymmetric design strategy for the partitioning of the IEDD-VQA dataset. Given that perception and recognition (L1), behavior description (L2), and physical quantization (L3) correspond directly to trajectory ground truths and possess unique, deterministic labels, they constitute the core of the training set. This approach aims to establish the model's precise cognition of the physical laws within driving scenarios through strong supervisory signals.

In contrast, counterfactual reasoning (L4) is inherently an open-ended causal prediction that lacks a unique physical ground truth as a supervisory signal. To prevent the introduction of uncertainty noise or the induction of model hallucinations during the training phase, the L4 reasoning task is reserved exclusively for the test set. This design establishes a challenging Out-of-Distribution (OOD) evaluation benchmark: it examines whether a model, after learning only objective physical facts ("what is involved" and "what happens"), can zero-shot derive hypothetical consequences based on its acquired physical common sense. Consequently, the test set contains complete L1–L4 task chains for 100 typical interaction scenarios, whereas the training set is strictly limited to objective factual descriptions (L1–L3).

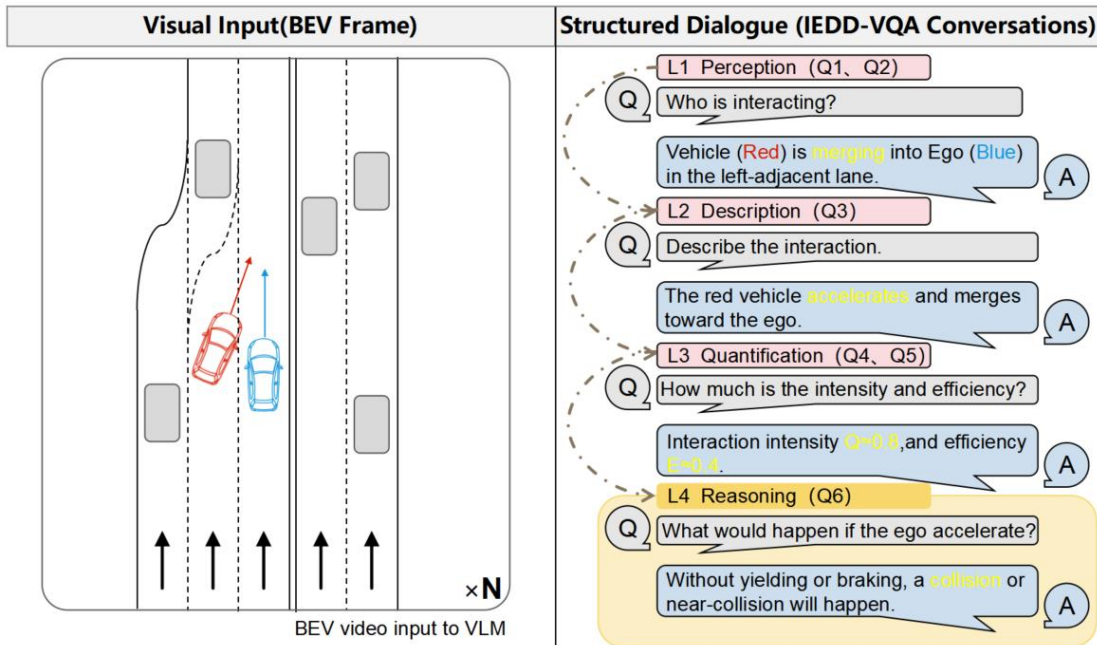


Fig 8. Task definitions and content examples of the IEDD-VQA dataset.

Technical Validation

To comprehensively evaluate the fine-grained understanding and reasoning capabilities of VLMs in the specialized domain of autonomous driving interactions, this study establishes a hierarchical and multi-dimensional evaluation framework. Mainstream models are rigorously assessed under three distinct experimental settings. This chapter elaborates on the experimental setup, the evaluation metric system, and the design rationale for the comparative experiments.

Experimental design

This section elaborates on the specific implementation details and evaluation criteria of the experiments. To ensure a fair comparison among VLM models with different architectures under a unified benchmark and to eliminate interference from data format discrepancies, the modal representation and preprocessing workflows for input data were first standardized. Subsequently, a hierarchical evaluation metric system was established across four dimensions—perception, description, quantization, and reasoning—aiming to comprehensively quantify the models' overall performance in interactive driving tasks.

(1) *Input representation and data preprocessing*

This experiment constructs a high-quality evaluation set comprising 100 typical interaction scenarios based on the IEDD-VQA test set. Considering the varying compatibility of different VLMs with video inputs, a unified multi-frame image sampling strategy is adopted to ensure the fairness and robustness of the evaluation. For each interaction segment:

- **Temporal Sampling:** Six key frames are uniformly extracted from the video to cover the entire temporal progression of the traffic interaction.
- **Image Preprocessing:** All images are resized to a fixed resolution (512×512) and Base64-encoded to preserve essential vehicle texture details while effectively managing token consumption.
- **Context Construction:** The 6-frame image sequence is utilized as a comprehensive visual context, provided as input only in the initial round of multi-turn dialogues. Subsequent question-answering relies entirely on the model's context retention capability.

(2) *Hierarchical and multi-dimensional evaluation metric system*

To comprehensively evaluate the perception, description, quantitative analysis, and reasoning capabilities of VLMs in autonomous driving scenarios, this study constructs a hierarchical evaluation framework. For each test sample, the evaluation system comprises four progressive levels and incorporates the LLM-as-a-Judge paradigm. A high-performance large language model, GLM-4.7, is utilized as the evaluator to score the physical rationality and safety of the generated content. These scores are ultimately aggregated into a Weighted Integrated Score (WIS).

(2.1) **Level 1: Perception and Identification** This level assesses the model's fundamental perception of key elements in traffic scenarios using two metrics:

- **Object ID Intersection over Union (Obj_IoU):** For the identification of key vehicles, the set of IDs extracted from the model's predicted text is compared with the ground-truth set to calculate the Intersection over Union (IoU).
- **Interaction Accuracy (Int_Acc):** This evaluates the accuracy of the model in classifying

vehicle interaction types.

(2.2)**Level 2: Action Description Quality** For the natural language description of driving behaviors, a dual evaluation standard of "semantic scoring + lexical overlap" is adopted:

- LLM Action Semantic Score (Act_Sem): The evaluator model assigns a score from 0 to 10 based on semantic consistency between the predicted text and the ground truth, focusing on "action correctness" and "hallucination-free generation." The score for this level is the normalized evaluator rating.

- Auxiliary Metric (ROUGE-L): The ROUGE-L (Recall-Oriented Understudy for Gisting Evaluation) score is calculated between the predicted and reference texts. Specifically, the F-measure based on the Longest Common Subsequence (LCS) is reported to quantify the lexical overlap between the generated text and the standard answer, compensating for the potential lack of granularity in pure semantic scoring.

(2.3)**Level 3: Quantitative and Logical Analysis** This level examines the model's numerical estimation capabilities and logical consistency regarding interaction intensity and efficiency parameters, primarily featuring:

- Mean Absolute Error (MAE): To intuitively measure the accuracy of physical parameter estimation, the average of the absolute differences between the predicted and ground-truth values across all test samples is calculated. This metric directly reflects the average deviation magnitude of the model at the physical scale; a lower value indicates more precise physical perception by the model.

$$MAE = \frac{1}{N} \sum_{i=1}^N |a_{gt}^i - a_{pred}^i| \quad (11)$$

- Logical Consistency (Log_Acc): This is a binary metric used to verify whether the model's judgment regarding the relative magnitudes of two physical quantities aligns with the ground truth. Rather than relying on specific numerical precision, this metric focuses on evaluating the model's logical reasoning capability regarding the interrelationships between objects in a scene.

When calculating the final score for this level (L3), to integrate the non-normalized MAE with the probabilistic logical consistency, the MAE is first mapped to a normalized score in the range of [0, 1] based on a tolerance threshold of 0.5. This score is then averaged with the logical consistency accuracy to represent the overall performance of this level.

(2.4)**Level 4: Counterfactual Reasoning** This level requires the model to address complex reasoning queries, such as predicting the consequences of alternative actions.

- Reasoning Quality Score (Reas_Score): The evaluator model focuses on the causal logic and safety boundary awareness of the reasoning process, with scores 0 - 10, then normalized to the [0,1] for WIS.

- Auxiliary Metric (ROUGE-L): Similar to Level 2, the F1-measure of ROUGE-L is calculated to evaluate the similarity between the generated reasoning text and expert-annotated answers regarding key terminology and phrasing.

(2.5)**Weighted Integrated Score (WIS)** To derive a single-point metric reflecting the model's comprehensive capability, the performance across the four levels is integrated via a weighted sum. First, the metrics for each level are normalized into scores L1 through L4 within the [0, 1] range. Considering that safety-critical long-tail reasoning is paramount in autonomous driving tasks, a higher weight is assigned to the reasoning level in the final WIS

calculation:

$$WIS=0.2 \cdot L1+0.2 \cdot L2+0.2 \cdot L3+0.4 \cdot L4 \quad (12)$$

The WIS ranges from 0 to 1, where a higher score indicates superior overall performance in autonomous driving interaction tasks.

Benchmark evaluation and analysis of mainstream VLMs

Based on the aforementioned hierarchical evaluation framework, this study selects several representative VLMs for a systematic evaluation. The experiments are designed to address two core questions: first, do general-purpose mainstream VLMs possess the fundamental capability to understand complex interaction scenarios without domain-specific fine-tuning in the autonomous driving field? Second, can prompt engineering strategies, such as CoT, effectively unlock the potential of these models in physical quantization and logical reasoning? This section begins by assessing zero-shot benchmark performance to analyze the distribution of strengths and weaknesses across different capability levels, followed by an exploration of the impact of prompting strategies on model performance.

(1) Zero-shot performance evaluation

To establish the baseline performance of the IEDD-VQA dataset, ten representative VLMs were selected for zero-shot evaluation. The evaluation subjects encompass a diverse range of architectures, from lightweight to large-scale parameters. Notably, this experiment includes three open-source models (Llama-4-Maverick, Qwen2.5-VL-7B, and GLM-4.6V), while the remainder are closed-source commercial models. As illustrated in Table 4 and Fig 9, the experimental results reveal significant performance differentiation and an intriguing "open-source counterattack" phenomenon.

Model	Overall	Percep	Percep	Descrip	Descrip	Qua	Qua	Reaso	Reaso
		tion	tion	tion	tion	nt.	nt.	ning	ning
	WIS	(L1)	(L1)	(L2)	(L2)	(L3)	(L3)	(L4)	(L4)
		Obj	Int	Act	ROUG	MA	Log	Reas	ROUG
		IoU	Acc	Sem	E	E	Acc	Score	E
seed-1.6-flash	0.1348	0.205	0.25	0.35	0.3048	1358.1	0.21	1.53	0.1529
kimi-k2.5 ⁵⁷	0.0964	0.2514	0.31	0.23	0.2495	650.8	0.21	0.36	0.1448
llama-4-maverick	0.342	0.2304	0.25	0.28	0.2311	714.3	0.43	4.93	0.0921
nova-2-lite-v1	0.1876	0.334	0.25	0.23	0.2246	1084.7	0.24	2.52	0.1019
glm-4.6v	0.1696	0.3592	0.27	0.27	0.2866	1359.4	0.25	1.91	0.156
claude-3-hai	0.0934	0.3183	0.3	0.73	0.2376	1283.3	0.11	0.14	0.1222
gemini-2.5-flash ⁵⁸	0.2091	0.3767	0.29	0.34	0.356	1352.7	0.39	2.42	0.1553
gpt-4o	0.2004	0.2958	0.35	0.26	0.2694	1358.1	0.21	2.74	0.1262

grok-4.1-fas t	0.16 12	0.2974	0.26	0.14	0.2257	136 0.6	0.44	1.47	0.1282
qwen2.5-vl- 7b	0.27 47	0.3795	0.24	0.31	0.2599	185 5.5	0.15	4.66	0.1195

Table 4. Zero-shot evaluation results of ten mainstream VLMs on IEDD-VQA

In terms of the Weighted Integrated Score (WIS), the open-source model Llama-4-Maverick ranked first with a score of 0.342, demonstrating exceptional comprehensive understanding of driving scenarios. It is followed by Qwen2.5-VL-7B (WIS=0.275), another open-source model, and the closed-source model Gemini-2.5-flash (WIS=0.209). In contrast, widely recognized closed-source flagship models such as GPT-4o (WIS=0.200) and Claude-3-Haiku (WIS=0.093) did not hold an advantage in zero-shot performance within this specialized domain. The radar charts in Fig 9 intuitively illustrate this trend: the three open-source models in the top row generally yield larger envelope areas across the perception (L1), description (L2), and reasoning (L4) dimensions compared to or on par with the closed-source models in the second row. These results provide robust evidence that in the specific vertical domain of autonomous driving interactions, well-optimized open-source models have the potential to rival or even exceed the performance of top-tier closed-source models.

However, all models exhibited a significant bottleneck in the quantitative analysis (L3) dimension. As indicated in Table 4, in the absence of fine-tuning, the Mean Absolute Error (MAE) for all models is generally extremely high (e.g., 1855.5 for Qwen2.5-VL-7B and 1358.1 for GPT-4o). This suggests that although general-purpose VLMs possess strong semantic comprehension, extracting precise physical metrics directly from BEV videos remains a critical challenge. General models struggle to establish a direct and accurate mapping between visual features and physical numerical values.

	WIS	Obj IoU	Int Acc	Act Sem	ROUGE	MAE	Log Acc	Reas Score	ROUGE
seed-1.6-flash	0.2941	0.123	0.27	0.28	0.2326	148.932	0.54	2.68	0.0992
kimi-k2.5 ⁵⁷	0.1483	0.1177	0.26	0.34	0.1629	1080.1333	0.41	1.5	0.0711
llama-4-maverick	0.346	0.0923	0.25	0.17	0.085	249.24	0.34	4.76	0.0435
nova-2-lite-v1	0.195	0.3247	0.2	0.17	0.0999	1116.2373	0.34	2.12	0.0632
glm-4.6v	0.2171	0.324	0.26	0.29	0.2737	1056.5553	0.38	2.34	0.119
claude-3-haiku	0.1407	0.3108	0.31	0.49	0.1431	1337.182	0.47	0.51	0.084
gemini-2.5-flash ⁵⁸	0.2226	0.3181	0.26	0.25	0.2561	100.1293	0.08	3.79	0.105
gpt-4o	0.2262	0.2671	0.29	0.16	0.2182	452.194	0.12	3.71	0.1211
grok-4.1-fast	0.2692	0.0429	0.24	0.4	0.0537	1135.1347	0.47	4.28	0.0391
qwen2.5-vl-7b	0.2887	0.3823	0.26	0.79	0.2071	9.7333	0.16	4.75	0.096

Table 5. Model performance evaluation results after introducing the CoT strategy

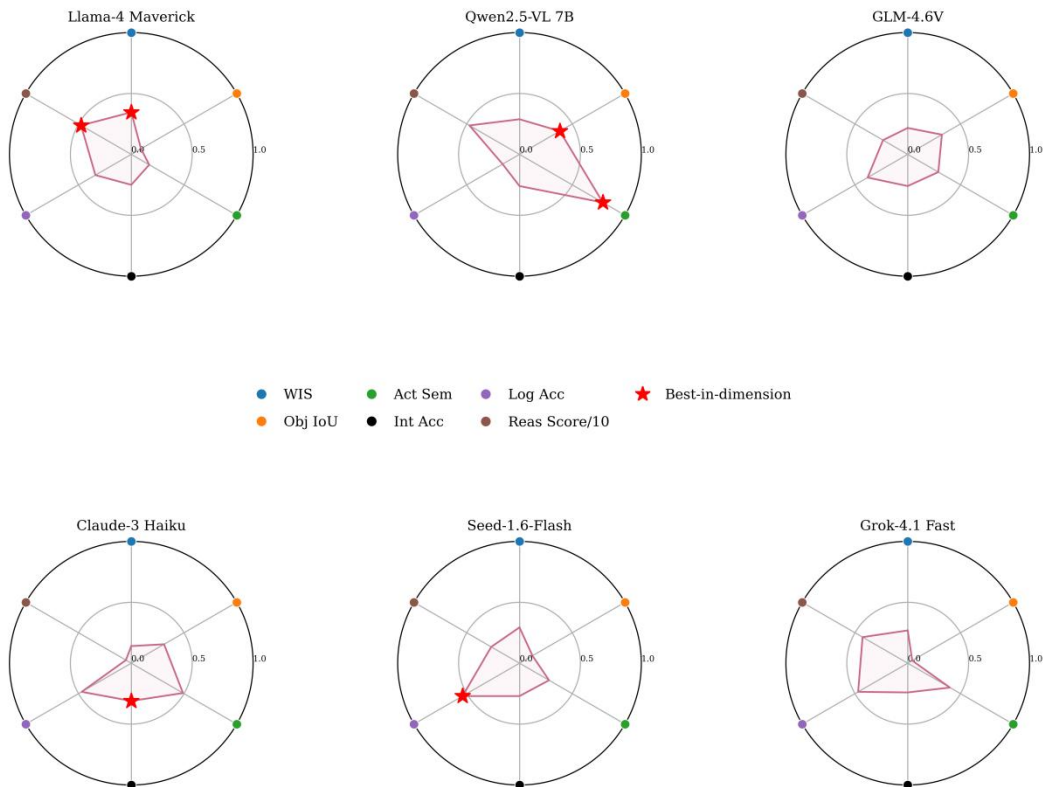


Fig 10. Radar charts of performance for selected models under the CoT strategy.



Fig 11. Heatmap illustrating performance gains across various metrics induced by the CoT strategy.

Domain-adaptive fine-tuning and ablation studies

To validate the value of the IEDD dataset in domain adaptation and explore methods for transforming general-purpose VLMs into expert-level driving interaction models, we conducted Low-Rank Adaptation (LoRA)⁵⁹ fine-tuning experiments on the top-performing open-source Qwen2.5-VL-7B based on the IEDD-VQA training set.

The experimental implementation was conducted using the PyTorch 2.6.0 and Parameter-Efficient Fine-Tuning (PEFT) 0.12.0 frameworks. We utilized two Xiyun C500 GPUs and employed the LoRA efficient fine-tuning strategy, with Qwen2.5-VL-7B-Instruct serving as the base model. To optimize training stability under constrained computational resources, the total training batch size was set to 128, achieved through 64 gradient accumulation steps. The AdamW optimizer was adopted with an initial learning rate of $5e-05$, supplemented by a cosine decay scheduling strategy and a warmup ratio of 0.05 to prevent gradient oscillations in the early stages of training. The model underwent training for 2 epochs on the IEDD-VQA training set, with the final validation loss converging to 0.0993. The loss convergence curve is depicted in Fig 12.

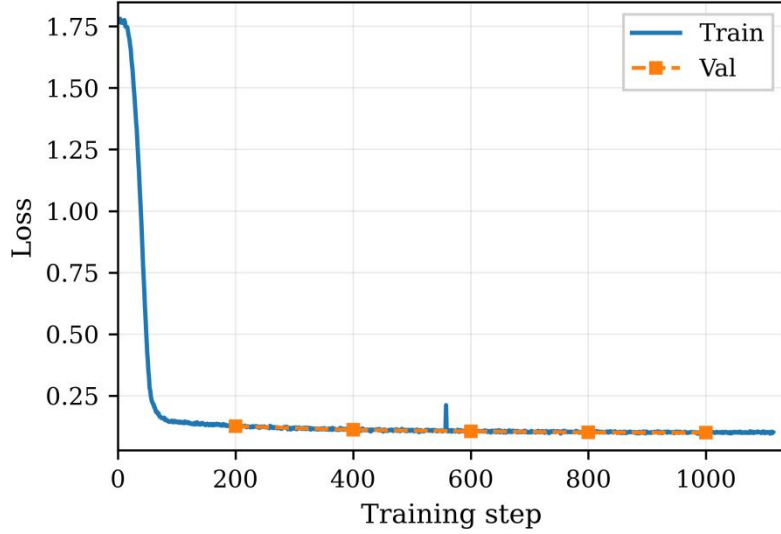


Fig 12. Training and validation loss convergence curves during the fine-tuning process.

Since the fine-tuning dataset solely covers perception (L1), description (L2), and quantification (L3) tasks and lacks targeted training for counterfactual reasoning (L4), this section employs the revised comprehensive metric WIS' for evaluation. Meanwhile, the L4 metric is retained to monitor the model's performance on OOD tasks.

$$WIS' = \frac{(L1+L2+L3)}{3} \quad (13)$$

Model	Over all	Percept ion (L1)	Percept ion (L1)	Descrip tion (L2)	Descrip tion (L2)	Quan t. (L3)	Qua nt. (L3)	Reason ing (L4)	Reason ing (L4)
	WIS'	Obj IoU	Int Acc	Act Sem	ROUG E	MAE	Log Acc	Reas Score	ROUG E
Baseline (Standard)	0.1475	0.3795	0.24	0.31	0.2599	1855.55	0.15	4.66	0.1195
Baseline + CoT	0.1644	0.3822	0.26	0.79	0.2071	9.73	0.16	4.75	0.096
Ours (Fine-tuned)	0.2636	0.3023	0.28	0.36	0.3005	0.3036	0.53	0.19	0.1511
Ours + CoT	0.2336	0.2838	0.25	0.32	0.2725	0.3704	0.52	0.37	0.1542

Table 6. Performance ablation study on in-distribution and out-of-distribution tasks before and after fine-tuning.

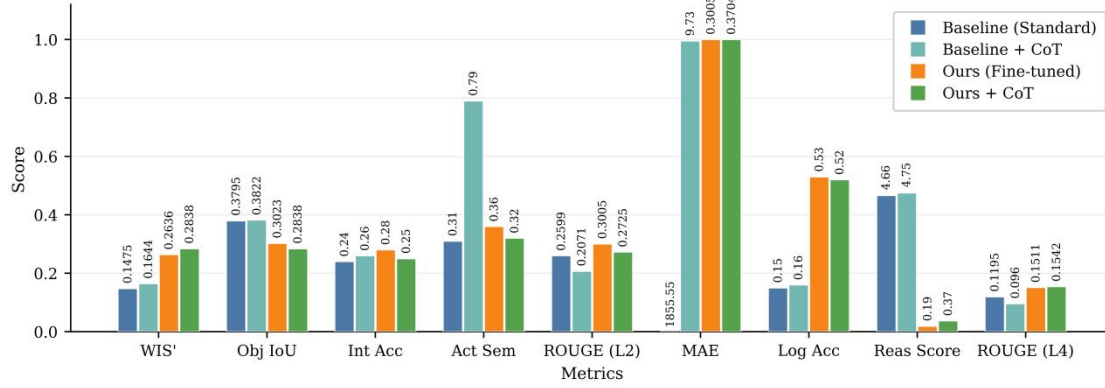


Fig 13. Detailed comparison bar chart of various evaluation metrics before and after fine-tuning.

The experimental results are presented in Table 6 and Fig 13. After fine-tuning on the IEDD-VQA dataset, the model (Ours) achieved significant performance gains across multiple core metrics, validating the effectiveness of domain-specific adaptation training:

- **Significant Enhancement in Overall Performance:** The revised weighted integrated score (WIS') of the fine-tuned model increased from 0.1475 (Baseline) to 0.2636, representing a 78.7% improvement. This result indicates that through targeted instruction fine-tuning, the model successfully bridged the domain gap between general-purpose scenarios and autonomous driving interactions, establishing stronger adaptability for in-distribution tasks.

- **Precision in Physical Perception and Quantification:** The most decisive breakthrough occurred at the L3 quantification level. Following fine-tuning, the Mean Absolute Error (MAE) converged sharply from an initial 1855.55 to 0.3036, while the logical accuracy (Log Acc) significantly improved from 0.15 to 0.53. This implies that the model not only mastered the semantic description of interactive scenarios but also accurately learned an internal representation mechanism that maps visual features to physical parameters such as speed and intensity, overcoming the inherent limitations of general-purpose models in numerical estimation.

- **Alignment of Action Semantics and Reversal of CoT Effects:** At the L2 description level, the action semantics score (Act Sem) steadily rose from 0.31 to 0.36, indicating that the generated descriptions of driving behavior aligned more closely with professional terminology. Notably, comparing the results of Ours (Fine-tuned) with Ours + CoT reveals that after sufficient fine-tuning, introducing CoT actually caused the WIS' to drop from 0.2636 back to 0.2336. This suggests that fine-tuning on the IEDD dataset has internalized complex interaction reasoning logic into the model's intuitive reactions; consequently, additional explicit reasoning steps may constitute information redundancy or interference, thereby reducing the quality of end-to-end outputs.

- **Trade-off Between Domain Specialization and General Capability:** However, the catastrophic forgetting effect brought by fine-tuning cannot be ignored. On the L4 counterfactual reasoning task, which was not included in the fine-tuning data, the reasoning score plummeted from a baseline of 4.66 to 0.19. This phenomenon underscores the limitations of LoRA fine-tuning in strengthening domain-specific capabilities: while the model becomes highly adapted to the specific instruction formats and physical ground truths of IEDD-VQA, it sacrifices the general logical reasoning capabilities and generalization

advantages for open-ended unknown scenarios acquired during the pre-training phase.

In summary, the IEDD dataset effectively transforms a general VLM into a "domain expert" focused on interactive perception and quantification, albeit at the cost of certain general cognitive abilities. This suggests that future research should incorporate broader task replay or regularization strategies during instruction fine-tuning to maintain robustness on OOD data while pursuing peak specialized performance.

Data availability

The complete dataset IEDD and IEDD-VQA is archived on Zenodo (<https://doi.org/10.5281/zenodo.18742437>). The raw data for the original datasets can be found in the corresponding literature or websites.

Code availability

The source code for IEDD is publicly available in a GitHub repository at: (<https://github.com/egik-von/IEDD>). The repository provides scripts to (i) prepare and load multi-dataset trajectories via trajdata caches, (ii) generate BEV vision clips and corresponding action semantics from the released CSV annotations (e.g., IEDD-traj2VisAct.py), (iii) construct ShareGPT-format VQA data (Q1–Q5) and augment counterfactual reasoning questions (Q6) to build the IEDD-VQA_test benchmark (e.g., IEDD-2vqa.py, IEDD-traj2Q6.py), and (iv) run model evaluation on the generated test set using OpenRouter-based inference (e.g., IEDD-benchmark.py).

References

1. Zhang X, Xiong L, Zhang P, et al. Real-world troublemaker: A 5g cloud-controlled track testing framework for automated driving systems in safety-critical interaction scenarios[J]. IEEE Internet of Things Journal, 2025.
2. Abdel-Aty M, Ding S. A matched case-control analysis of autonomous vs human-driven vehicle accidents[J]. Nature communications, 2024, 15(1): 4931.
3. Yu R, Li Z, Xiong L, et al. Uncertainty-Aware Safety-Critical Decision and Control for Autonomous Vehicles at Unsignalized Intersections[J]. arXiv preprint arXiv:2505.19939, 2025.
4. Yang Y, Han C, Mao R, et al. Survey of General End-to-End Autonomous Driving: A Unified Perspective[J]. Authorea Preprints, 2025.
5. Xu Y, Hu Y, Zhang Z, et al. Vlm-ad: End-to-end autonomous driving through vision-language model supervision[J]. arXiv preprint arXiv:2412.14446, 2024.
6. Tian X, Gu J, Li B, et al. Drivevlm: The convergence of autonomous driving and large vision-language models[J]. arXiv preprint arXiv:2402.12289, 2024.
7. Xie C, Sun B, Li T, et al. LatentVLA: Efficient Vision-Language Models for Autonomous Driving via Latent Action Prediction[J]. arXiv preprint arXiv:2601.05611, 2026.
8. Li P, Zheng Y, Wang Y, et al. Discrete diffusion for reflective vision-language-action models in autonomous driving[J]. arXiv preprint arXiv:2509.20109, 2025.

9. Cao J, Zhang Q, Jia P, et al. Fastdrivevla: Efficient end-to-end driving via plug-and-play reconstruction-based token pruning[J]. arXiv preprint arXiv:2507.23318, 2025.
10. Hwang J J, Xu R, Lin H, et al. Emma: End-to-end multimodal model for autonomous driving[J]. arXiv preprint arXiv:2410.23262, 2024.
11. Xie Y, Xu R, He T, et al. S4-driver: Scalable self-supervised driving multimodal large language model with spatio-temporal visual representation[C]//Proceedings of the IEEE/CVF Conference on Computer Vision and Pattern Recognition (CVPR). Nashville, USA: IEEE, 2025: 1622-1632.
12. Seff A, Cera B, Chen D, et al. Motionlm: Multi-agent motion forecasting as language modeling[C]//Proceedings of the IEEE/CVF International Conference on Computer Vision (ICCV). Paris, France: IEEE, 2023: 8579-8590.
13. Punzo V, Borzacchiello M T, Ciuffo B. On the assessment of vehicle trajectory data accuracy and application to the Next Generation SIMulation (NGSIM) program data[J]. Transportation Research Part C: Emerging Technologies, 2011, 19(6): 1243-1262.
14. Caesar H, Bankiti V, Lang A H, et al. nuScenes: A multimodal dataset for autonomous driving[C]//Proceedings of the IEEE/CVF Conference on Computer Vision and Pattern Recognition (CVPR). Seattle, WA, USA: IEEE, 2020: 11621-11631.
15. Houston J, Zuidhof G, Bergamini L, et al. One thousand and one hours: Self-driving motion prediction dataset[C]//Proceedings of the 4th Conference on Robot Learning (CoRL). Cambridge, MA, USA: PMLR, 2021: 409-418.
16. Sun P, Kretschmar H, Dotiwalla X, et al. Scalability in perception for autonomous driving: Waymo open dataset[C]//Proceedings of the IEEE/CVF Conference on Computer Vision and Pattern Recognition (CVPR). Seattle, WA, USA: IEEE, 2020: 2446-2454.
17. Liu H X, Feng S. Curse of rarity for autonomous vehicles[J]. nature communications, 2024, 15(1): 4808.
18. Geiger A, Lenz P, Urtasun R. Are we ready for autonomous driving? The KITTI vision benchmark suite[C]//Proceedings of the IEEE Conference on Computer Vision and Pattern Recognition (CVPR). Providence, RI, USA: IEEE, 2012: 3354-3361.
19. Yu F, Chen H, Wang X, et al. BDD100K: A diverse driving dataset for heterogeneous multitask learning[C]//Proceedings of the IEEE/CVF Conference on Computer Vision and Pattern Recognition (CVPR). Seattle, WA, USA: IEEE, 2020: 2636-2645.
20. Mao J, Niu M, Jiang C, et al. One million scenes for autonomous driving: Once dataset[J]. arXiv preprint arXiv:2106.11037, 2021.
21. Sima C, Renz K, Chitta K, et al. DriveLM: Driving with graph visual question answering[C]//Proceedings of the European Conference on Computer Vision (ECCV). Milan, Italy: Springer Nature Switzerland, 2025: 256-274.
22. Wang W, Xie J, Hu C Y, et al. Drivemlm: Aligning multi-modal large language models with behavioral planning states for autonomous driving[J]. arXiv preprint arXiv:2312.09245, 2023.
23. Mao J, Qian Y, Ye J, et al. Gpt-driver: Learning to drive with gpt[J]. arXiv preprint arXiv:2310.01415, 2023.
24. Mao J, Ye J, Qian Y, et al. A language agent for autonomous driving[J]. arXiv preprint arXiv:2311.10813, 2023.
25. Dosovitskiy A, Ros G, Codevilla F, et al. CARLA: An open urban driving

simulator[C]//Proceedings of the 1st Conference on Robot Learning (CoRL). Mountain View, CA, USA: PMLR, 2017: 1-16.

26. Gaidon A, Wang Q, Cabon Y, et al. Virtual worlds as proxy for multi-object tracking analysis[C]//Proceedings of the IEEE Conference on Computer Vision and Pattern Recognition (CVPR). Las Vegas, NV, USA: IEEE, 2016: 4340-4349.

27. Jiang, X., Zhao, X., Liu, Y. et al. A naturalistic trajectory dataset with dense interaction for autonomous driving. *Sci Data* 12, 1084 ,2025. <https://doi.org/10.1038/s41597-025-05344-7>

28. Chen C, Liu Z, Liang W, et al. PODAR: A collision risk model offering valid signals for vehicular interactions[J]. *IEEE Intelligent Transportation Systems Magazine*, 2025.

29. Chang C, Zhang J, Ge J, et al. VistaScenario: Interaction scenario engineering for vehicles with intelligent systems for transport automation[J]. *IEEE Transactions on Intelligent Vehicles*, 2024.

30. Van Der Horst R. Time-to-collision and collision avoidance systems[J]. 1994.

31. Hayward J C. Near miss determination through use of a scale of danger[J]. 1972.

32. Gettman D, Head L. Surrogate safety measures from traffic simulation models[J]. *Transportation research record*, 2003, 1840(1): 104-115.

33. Allen B L, Shin B T, Cooper P J. Analysis of traffic conflicts and collisions[R]. 1978.

34. Lu D, Du H, Wu Z, et al. Risk assessment in autonomous driving: a comprehensive survey of risk sources, methodologies, and system architectures[J]. *Autonomous Intelligent Systems*, 2025, 5(1): 24.

35. Riedmaier S, Ponn T, Ludwig D, et al. Survey on scenario-based safety assessment of automated vehicles[J]. *IEEE access*, 2020, 8: 87456-87477.

36. Caesar H, Kabzan J, Tan K S, et al. nuplan: A closed-loop ml-based planning benchmark for autonomous vehicles[J]. *arXiv preprint arXiv:2106.11810*, 2021.

37. Chang M F, Lambert J, Sangkloy P, et al. Argoverse: 3D tracking and forecasting with rich maps[C]//Proceedings of the IEEE/CVF Conference on Computer Vision and Pattern Recognition (CVPR). Long Beach, CA, USA: IEEE, 2019: 8748-8757.

38. Wilson B, Qi W, Agarwal T, et al. Argoverse 2: Next generation datasets for self-driving perception and forecasting[J]. *arXiv preprint arXiv:2301.00493*, 2023.

39. Krajewski R, Bock J, Kloeker L, et al. The highD dataset: A drone dataset of naturalistic vehicle trajectories on German highways for validation of highly automated driving systems[C]//Proceedings of the 21st International Conference on Intelligent Transportation Systems (ITSC). Maui, HI, USA: IEEE, 2018: 2118-2125.

40. Bock J, Krajewski R, Moers T, et al. The inD dataset: A drone dataset of naturalistic road user trajectories at German intersections[C]//Proceedings of the IEEE Intelligent Vehicles Symposium (IV). Las Vegas, NV, USA: IEEE, 2020: 1929-1934.

41. Zhan W, Sun L, Wang D, et al. Interaction dataset: An international, adversarial and cooperative motion dataset in interactive driving scenarios with semantic maps[J]. *arXiv preprint arXiv:1910.03088*, 2019.

42. Xu Y, Shao W, Li J, et al. SIND: A drone dataset at signalized intersection in China[J]. *arXiv preprint arXiv:2209.02297*, 2022.

43. Kim J, Rohrbach A, Darrell T, et al. Textual explanations for self-driving vehicles[C]//Proceedings of the European Conference on Computer Vision (ECCV). Munich,

Germany: Springer, 2018: 563-578.

44. Malla S, Choi C, Dwivedi I, et al. DRAMA: Joint risk localization and captioning in driving[C]//Proceedings of the IEEE/CVF Winter Conference on Applications of Computer Vision (WACV). Waikoloa, HI, USA: IEEE, 2023: 1043-1052.

45. Qian T, Chen J, Zhuo L, et al. NuScenes-QA: A multi-modal visual question answering benchmark for autonomous driving scenario[C]//Proceedings of the AAAI Conference on Artificial Intelligence (AAAI). Vancouver, Canada: AAAI Press, 2024, 38(5): 4542-4550.

46. Nie M, Peng R, Wang C, et al. Reason2Drive: Towards interpretable and chain-based reasoning for autonomous driving[C]//Proceedings of the European Conference on Computer Vision (ECCV). Milan, Italy: Springer Nature Switzerland, 2025: 292-308.

47. Wei J, Wang X, Schuurmans D, et al. Chain-of-thought prompting elicits reasoning in large language models[J]. Advances in neural information processing systems, 2022, 35: 24824-24837.

48. Guo X, Zhang R, Duan Y, et al. Surds: Benchmarking spatial understanding and reasoning in driving scenarios with vision language models[J]. arXiv preprint arXiv:2411.13112, 2024.

49. Chi H, Gao H, Liu Z, et al. Impromptu vla: Open weights and open data for driving vision-language-action models[J]. arXiv preprint arXiv:2505.23757, 2025.

50. Hao Y, Li Z, Sun L, et al. Driveaction: A benchmark for exploring human-like driving decisions in vla models[J]. arXiv preprint arXiv:2506.05667, 2025.

51. Kharlamova A, Liu J, Zhang T, et al. LLM-Driven Kernel Evolution: Automating Driver Updates in Linux[J]. arXiv preprint arXiv:2511.18924, 2025.

52. Zhao Z, Fu H, Liang D, et al. Extending large vision-language model for diverse interactive tasks in autonomous driving[J]. arXiv preprint arXiv:2505.08725, 2025.

53. Marcu A M, Chen L, Hünemann J, et al. LingoQA: Visual question answering for autonomous driving[C]//Proceedings of the European Conference on Computer Vision (ECCV). Milan, Italy: Springer Nature Switzerland, 2025: 252-269.

54. Ma Y, Cui C, Cao X, et al. LaMPilot: An open benchmark dataset for autonomous driving with language model programs[C]//Proceedings of the IEEE/CVF Conference on Computer Vision and Pattern Recognition (CVPR). Seattle, WA, USA: IEEE, 2024: 15141-15151.

55. Chen L, Sinavski O, Hünemann J, et al. Driving with LLMs: Fusing object-level vector modality for explainable autonomous driving[C]//Proceedings of the IEEE International Conference on Robotics and Automation (ICRA). Yokohama, Japan: IEEE, 2024: 14093-14100.

56. Fang J, Li L, Zhou J, et al. Abductive ego-view accident video understanding for safe driving perception[C]//Proceedings of the IEEE/CVF Conference on Computer Vision and Pattern Recognition (CVPR). Seattle, WA, USA: IEEE, 2024: 22030-22040.

57. Team K, Bai T, Bai Y, et al. Kimi K2. 5: Visual Agentic Intelligence[J]. arXiv preprint arXiv:2602.02276, 2026.

58. Comanici G, Bieber E, Schaekermann M, et al. Gemini 2.5: Pushing the frontier with advanced reasoning, multimodality, long context, and next generation agentic capabilities[J]. arXiv preprint arXiv:2507.06261, 2025.

59. Hu E J, Shen Y, Wallis P, et al. Lora: Low-rank adaptation of large language models[J]. Iclr, 2022, 1(2): 3.

Funding

This work is supported by the National Key Research and Development Program of China under Grants 2024YFB2505704 and the National Natural Science Foundation of China under Grants 52325212.

Author contributions

Haojie Feng proposed the novel framework, developed the data generation pipeline, and wrote the original draft. Peizhi Zhang provided theoretical guidance on the methodology and supervised the overall research design. Mengjie Tian and Xinrui Zhang assisted in data processing and prepared the visualization figures. Zhuoren Li contributed to the conceptualization of the interaction metrics and managed the dataset curation process. Junpeng Huang and Xiurong Wang performed the technical validation and analyzed the experimental results. Junfan Zhu and Jianzhou Wang contributed to the discussions on synthetic data and autonomous driving VLMs. Dongxiao Yin and Lu Xiong supervised the project administration and dataset organization. All authors discussed the results and contributed to the final manuscript.

Competing interests

The authors declare no competing interests.